Infrared Lattice Bands in AlSb

W. J. TURNER AND W. E. REESE
International Buisness Machines, Thomas J. Watson Research Center, Yorktown Heights, New York
(Received February 12, 1962)

Lattice bands in AlSb involving interactions of infrared radiation with one, two, three, and four phonons have been observed between 8 and 38 μ. The multiphonon combination bands (summation or difference) can be explained in terms of four characteristic phonons at or near the zone boundary. The corresponding phonon wave numbers are 316, 297, 132, and 65 cm^{-1}. The interaction of infrared radiation with the transverse optical phonon at the center of the zone results in a single-phonon absorption band and the Reststrahlen reflectivity band. The reflectivity data can be fitted to simple dispersion theory. The fundamental optical frequency from this fit is $(9.564\pm0.019)\times10^{12}$ sec^{-1} (319 cm^{-1}). The index of refraction n and extinction coefficient k were calculated as functions of wavelength between 20 and 38 μ using dispersion theory.

1. INTRODUCTION

INFRARED lattice absorption bands attributed to multiphonon combinational (summation or difference) bands have been reported for Ge,[1] Si,[2] GaP,[3,4] InSb,[5] SiC,[6] and GaAs.[7] These bands arise from the direct interaction of infrared radiation with phonons in the crystal lattice. For heteropolar crystals the mechanism of interaction has usually been assumed[8] to be the anharmonic part of the crystal potential. The combinational bands are part of the fundamental resonance absorption in this case, because the interaction of the crystal with the radiation takes place through the dipole moment of the fundamental oscillations. A photon is absorbed and through an intermediate state in which the fundamental oscillation is excited, two phonons are created, neither of which is a fundamental phonon. For homopolar crystals such as germanium and silicon this mechanism could not operate since the fundamental resonance has no dipole moment. To explain the observed absorption in such cases Lax and Burnstein[9] have suggested that two phonons can interact directly with the radiation field through terms in the electric moment of second order in the atomic displacements. Terms in the electric moment of higher order in the atomic displacements can result in higher-order processes such as three of four phonon processes. The order of the term in the electric moment corresponds to the number of phonons involved. The second (or higher order) electric-moment mechanism may be important in heteropolar crystals and in ionic crystals as well as in homopolar crystals. In InSb, for example, one-, two-, and three-phonon bands have been found and explained in terms of this mechanism.[5] However, for GaP, Kleinman[4] has shown that the results of Kleinman and Spitzer[3] can be explained in terms of the anharmonic forces mechanism. Both mechanisms predict the same temperature dependence[4] and essentially the same shape for the absorption which is determined primarily by the frequency distribution of the lattice vibrations. In general, only in the homopolar case is the mechanism established for the combination bands.

Two distinct types of interaction are possible: First, summation bands exist in which a photon is absorbed and two or more phonons are emitted. Second, difference bands exist in which a photon and one or more low-energy phonons are absorbed and one or more high-energy phonons are emitted. These two processes have different temperature dependences. The net probability of absorption in each case will be the difference between the probability of the absorption of a photon with the emission and absorption of phonons and the probability of stimulated emission of a photon with the absorption and emission of phonons. The temperature dependence of the optical process involving the emission of a phonon of wave number $\bar{\nu}_p$ is $1+F_p$ while the temperature dependence of the optical process involving the absorption of a phonon is F_p, where $F_p=[\exp(hc\bar{\nu}_p/kT)-1]^{-1}$. Thus, for example, for a two-phonon summation band the temperature dependence of the net power absorbed is $(1+F_1)(1+F_2)-F_1F_2$ while for a two-phonon difference band the factor is $(1+F_1)F_2-(1+F_2)F_1$. In each expression the first term is proportional to the probability of absorption of a photon and the second term is proportional to the probability of stimulated emission of a photon. For low-temperature or high-energy phonons, the summation bands will be most probable.

In all these interactions the energy $h\nu$ and the wave vector k of the photon must be conserved. These conditions are given by

$$h\nu=\sum_p(\pm hc\bar{\nu}_p), \tag{1}$$

$$\mathbf{k}+n\mathbf{K}=\sum_p\pm\mathbf{q}_p, \tag{2}$$

where $hc\bar{\nu}_p$ and $\mathbf{q}_p$ are the energy and wave vector of the pth phonon of wave number $\bar{\nu}_p$ (positive sign is for emission and negative sign for absorption), $\mathbf{K}$ is a

[1] B. N. Brockhouse and P. K. Iyengar, Phys. Rev. **111**, 747 (1958).
[2] F. A. Johnson, Proc. Phys. Soc. (London) **73**, 265 (1959).
[3] D. A. Kleinman and W. G. Spitzer, Phys. Rev. **118**, 110 (1960).
[4] D. A. Kleinman, Phys. Rev. **118**, 118 (1960).
[5] S. J. Fray, F. A. Johnson, and R. H. Jones, Proc. Phys. Soc. (London) **76**, 939 (1960).
[6] L. Patrick and W. J. Choyke, Phys. Rev. **123**, 813 (1961).
[7] W. Cochran, S. J. Fray, F. A. Johnson, J. E. Quarrington, and N. Williams, Suppl. J. Appl. Phys. **32**, 2102 (1961).
[8] M. Born and M. Blackman, Z. Physik **82**, 551 (1933); M. Blackman, *ibid.* **86**, 421 (1933); Phil. Trans. Roy. Soc. London **A226**, 102 (1936); L. L. Barnes, R. R. Brattain, and F. Seitz, Phys. Rev. **48**, 582 (1935).
[9] M. Lax and E. Burstein, Phys. Rev. **97**, 39 (1955).

reciprocal lattice vector, and n is an integer, positive, negative, or zero. Since the wave vector of the photon is small compared to the phonon wave vector $\mathbf{q}_p$, the second condition becomes

$$n\mathbf{K}=\sum_p(\pm\mathbf{q}_p).$$

For one- and two-phonon processes $n=0$, while for a three-phonon process $n=0,\pm1$. Thus, in a single-phonon, interaction the phonon must be a zero-wave-vector phonon, i.e., a center-of-the-zone phonon. In a two-phonon summation band the above condition requires $\mathbf{q}_1=-\mathbf{q}_2$ while for a difference band $\mathbf{q}_1=\mathbf{q}_2$.

While the combination bands are a continuous absorption, absorption peaks occur because of singularities in the phonon frequency distribution. These singularities arise from critical points in the Brillouin zone where the curves of frequency as a function of wave vector for the individual branches are flat. Such points are expected to occur at or near the edge of the Brillouin zone. For a given phonon branch this flattening of the frequency as a function of phonon wave number makes it possible to characterize that branch by a single frequency. If the energy at the Brillouin zone boundary depends strongly on the wave vector direction, the combination band will be broadened by the broadening of the phonon distribution function and structure may also be introduced into the band.

2. EXPERIMENTAL

Some 20 samples of both p- and n-type AlSb were cut and optically polished to thicknesses between 0.75 and 0.0040 cm. This wide range of thickness was necessary because of the large range of absorption coefficients which were measured. The transmission and reflection of these samples were measured at 300 and 78°K in the spectral range of 8–38 μ. Two different spectrometers were used in the measurements. A modified Perkin Elmer model 21 double beam spectrophotometer was used for many of the measurements. In this instrument the sample was placed in a metal sample Dewar at a focal point in the polychromatic beam. Two prisms, NaCl and CsBr, were used to cover the desired wavelength range. A Reststrahlen filter was introduced at long wavelengths which reduced stray light to 0.2%. With a simple change of mirrors either transmission or reflection measurements could be made.

For higher resolution transmission studies a Perkin-Elmer 112 system with monochromatic sampling was utilized. NaCl, KBr, CsI prisms allowed measurements through the entire range. To decrease water vapor and CO_2 absorption, both instruments were flushed with dry nitrogen.

3. RESULTS AND DISCUSSION OF THE ABSORPTION STUDIES

The transmission and reflection coefficients of an optically-polished plane-parallel sample of thickness x, bulk reflectivity R, and absorption coefficient K are given by Eqs. (3) and (4)

$$T=(1-R)^2e^{-Kx}/(1-R^2e^{-2Kx}), \tag{3}$$

$$R'=R+TRe^{-Kx}. \tag{4}$$

These equations include multiple reflections but neglect interference effects. Using Eqs. (3) and (4), the optical absorption coefficients as a function of wavelength were calculated by a computer from the transmission and reflection data.

Figure 1 is a composite curve of absorption coefficient K in cm,$^{-1}$ plotted vs wavelength in microns for AlSb at 300°K. The curve results from data on several thicknesses of a n-type sample with an electron concentration of 7×10^{16} cm^{-3}. Absorption coefficient data from other crystals were similar but modified by different amounts of free carrier absorption. The absorption peaks in the curve are due to the lattice absorption involving one, two, three, and four phonons. The strongest absorption band is the one which increases beyond the scale of the figure and reaches a maximum at 31.37 ± 0.5 μ. The maximum of this absorption was determined from an analysis of the Reststrahlen reflection band which occurs in this region as will be discussed below. This absorption arises from the absorption of a photon and the emission of a fundamental transverse optical phonon (TO_c) having zero wave vector, i.e., a phonon at the center of the zone. Seven bands are noted on the curve of Fig. 1. These are two-phonon summation bands which result when a photon is absorbed and two phonons of equal and opposite wave vector are emitted. The bands have wavelengths of 15.80, 16.31, 16.81, 22.33, 23.29, 26.30, and 27.50 μ. The 15.80 band which is labeled $2LO$ is seen only as a shoulder. At 77°K with high resolution, the peak is clearly resolved as shown in Fig. 2. The solid curve is for 300°K while the dashed curve is the curve for 77°K corrected for background contributions. The peaks shift toward higher wave numbers (shorter wavelengths) by 5 cm^{-1} at 77°K. Using these data the positions of the 300°K triplet $2LO$, $LO+TO$, and $2TO$ were established, hence, the

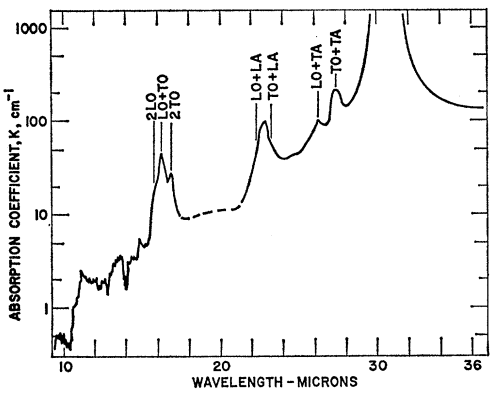

FIG. 1. Absorption coefficient of AlSb vs wavelength at 300°K.

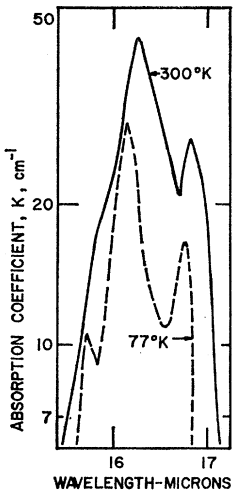

FIG. 2. Absorption triplet of the two optical phonons in AlSb at 300° and 77°K (dashed).

wave numbers corresponding to *LO* and *TO* were determined. The observed peak at 22.80 has two shoulders at 22.33 and 23.29. It is assumed that the single peak is actually a doublet corresponding to the shoulders involving *LO*+*LA* at 22.33 and *TO*+*LA* at 23.29. From these lines, knowing *LO* and *TO*, the wave number value of *LA* was determined. Even with the highest resolution available the doublet could not be resolved at 300 or 77°K. This may result from the lack of a broad flat region in the frequency vs wave vector curve for the *LA* branch. In other words there are no sharp maxima in the density in energy of the phonon states of the *LO*+*LA* and *TO*+*LA* branches. Therefore, the two bands are not sharply defined. The next two bands at 26.30 and 27.50 μ were attributed to *LO*+*TA* and *TO*+*TA*, respectively. From these bands the value of *TA* was obtained. Table I gives the values of the 4 characteristic phonons *LO*, *TO*, *LA*, *TA* in units of wave number cm^{-1}, temperature °K, and energy in eV which were determined from the two-phonon bands. It should be noted that the assignment of the two optical phonons was quite arbitrary. At the center of the zone in an ionic crystal, *LO* would be greater than *TO* according to the Lyddane-Sachs-Teller relation[10] as noted in Sec. 4. At the zone boundary it has been assumed that *LO* is also larger than *TO* as Kleinman and Spitzer[3] have done for GaP. Other authors, e.g., Fray *et al.*[5] for InSb and Cochran *et al.*[7] for GaAs, believe that *LO* and *TO* branches cross in these materials making *TO* greater than *LO* at the zone boundary. Neutron scattering experiments such as those performed by Brockhouse and Iyengar[1] on germanium provide the most direct way of determining the spectrum of the phonon frequencies as functions of the phonon wave vectors for the individual branches. For the acoustical branches, *LA* has been found to be larger than *TA* for other materials and this has been assumed to be the case in AlSb.

TABLE I. The four characteristic phonons of AlSb given in different units.

	$\bar{\nu}$ (cm^{-1})	(°K)	(eV)
LO	316	454	0.039
TO	297	428	0.037
LA	132	190	0.016
TA	65	93	0.008

[10] R. H. Lyddane, R. G. Sachs, and E. Teller, Phys. Rev. **59**, 673 (1941).

The temperature dependence of the net power absorbed in a two-phonon summation band was given in the introduction as

$$(1+F_1)(1+F_2)-F_1F_2, \tag{5}$$

which simplifies to

$$1+F_1+F_2, \tag{6}$$

where

$$F_p=[\exp(hc\bar{\nu}_p/kT)-1]^{-1} \tag{7}$$

and $\bar{\nu}_p$=wave number of the pth phonon. The temperature factor f will be defined as the ratio of the magnitudes of the lattice band at 300 and 77°K. From the above equations the expected temperature factor f_c, is

$$f_c=(1+F_1+F_2)_{300°K}/(1+F_1+F_2)_{77°K}. \tag{8}$$

In order to determine the observed temperature factor f_o, it was necessary to correct the value of the absorption coefficient at the peak for the background due to free carrier absorption or impurity absorption and the tail of the fundamental single phonon (TO_c) absorption. In essence this correction involves subtraction of background from the peak heights for the two temperatures. Table II gives a summary of the two-phonon summation band data and the proposed assignments. The observed and expected values of band wavelength in microns, wave numbers in cm^{-1}, and temperature factor f are given. The values for the four characteristic phonons given in Table I give agreement between expected and observed two-phonon wave numbers of 1 cm^{-1} or better. The predicted and observed temperature factors are also in good agreement.

Referring back to Fig. 1, several bands are apparent at wavelengths shorter than the 2*LO* or 15.8 μ band. These bands are three- and four-phonon bands. Figure 3 shows this region in detail. The three-phonon bands

TABLE II. Summary of the two-phonon summation band data for AlSb with proposed assignment.

Observed				Expected		
$\lambda(\mu)$	$\bar{\nu}$ (cm^{-1})	f_o	Assignment	$\lambda(\mu)$	$\bar{\nu}$ (cm^{-1})	f_c
15.80	633	1.56	2*LO*	15.82	632	1.55
16.31	613	1.57	*LO*+*TO*	16.31	613	1.59
16.81	595	1.70	2*TO*	16.83	594	1.62
22.33	448	1.91	*LO*+*LA*	22.32	448	2.20
23.29	429	2.27	*TO*+*LA*	23.31	429	2.23
26.30	380	2.86	*LO*+*TA*	26.25	381	2.82
27.50	363	2.83	*TO*+*TA*	27.62	362	2.84

are indicated by letters and the four-phonon by numbers. Using the same four characteristic wave numbers obtained from the two-phonon bands, the three- and four-phonon band assignments along with the expected and observed values of wavelength and wave numbers are shown in Table III. Thirty-eight bands are identified and for all but one the agreement between the observed and the expected wave number values is 3 cm^{-1} or better. The maximum discrepancy is only 4 cm^{-1}. Even in this case an error of 1 cm^{-1} per phonon would explain such a discrepancy since four phonons are involved. Since the agreement is generally better than this, the values of the four characteristic phonons are considered good. The relative magnitudes of the lattice bands of Figs. 1 and 3 are reasonable. The order of magnitude values of the absorption coefficients for the various bands are 0.5 cm^{-1} for four-phonon, 3 cm^{-1} for three-phonon, 50 cm^{-1} for two-phonon, and orders of magnitude greater for the single-fundamental phonon band. Thus when more than one process contributed, the absorption level was given by the process involving the least number of phonons. In the region of 17.5–21 μ (dashed region in Fig. 1) several three- and four-phonon bands exist but the presence of the much larger two-phonon bands on each side of it made getting reliable data difficult. Since no really new information would be added, this region was not studied extensively except on one sample which indicated in agreement with the expected results.

4. ANALYSIS OF THE RESTSTRAHLEN BAND

The partially ionic nature of AlSb gives an optically-active fundamental lattice vibration viz TO_c phonon. As previously noted, this results in a large absorption band. It also gives rise to a dispersive reflection band known as the Reststrahlen band. The reflectivity of AlSb was measured throughout the Reststrahlen region on a thick sample (0.75 cm) which was lapped on one side and optically polished and etched on the other side. The reflection curve was fitted to classical dispersion theory. The method used was similar to that used by Spitzer and Kleinman[11] for SiC and Kleinman and Spitzer[3] for GaP. An IBM 7090 program was written which adjusted four parameters ($\epsilon_0,\nu_0,\rho,\gamma$) for the best least-squares fit of the data to a single resonance. The reflectivity of AlSb vs wavelength in microns is shown in Fig. 4. The theoretical curve is shown as a solid line while the points are the experimental data. The fit is within the accuracy of the reflection measurement except at the region of the minimum and maximum. Here the difference is only 2% and is probably a result of imperfect or partially oxidized surface. The values obtained from this fit are

$$\begin{aligned}\nu_0&=(9.564\pm0.019)\times10^{12}\ \text{sec}^{-1},\\ \lambda_0&=31.37\pm0.05\ \mu,\\ \rho&=0.1060\pm0.0005,\\ \gamma&=0.0059\pm0.0005,\\ \epsilon_0&=9.880\pm0.2,\end{aligned}\tag{9}$$

TABLE III. Summary of the three- and four-phonon combination bands in AlSb.

Line	No.	Assignment	Expected $\bar{\nu}$ (cm^{-1})	Expected $\lambda(\mu)$	Observed $\bar{\nu}$ (cm^{-1})	Observed $\lambda(\mu)$
	1	$3LO+LA$	1080	9.26	1081	9.26
	2	$2LO+TO+LA$	1061	9.42	1059	9.44
	3	$LO+2TO+LA$	1042	9.60	1042	9.60
	4	$3TO+LA$	1023	9.77	1023	9.77
	5	$3LO+TA$	1013	9.87	1012	9.88
	6	$2LO+TO+TA$	994	10.06	996	10.03
	7	$2TO+LO+TA$	975	10.26	975	10.26
	8	$3TO+TA$	956	10.46	959	10.43
A		$3LO$	948	10.55	949	10.54
B		$2LO+TO$	929	10.76	928	10.78
C		$LO+2TO$	910	10.99	911	10.98
	9	$2LO+2LA$	896	11.16	896	11.16
D		$3TO$	891	11.22	893	11.20
	10	$3LO-TA$	883	11.32	883	11.33
	11	$LO+TO+2LA$	877	11.40	876	11.42
	12	$2LO+TO-TA$	864	11.57	865	11.56
	13	$2TO+2LA$	858	11.65	858	11.65
	14	$LO+2TO-TA$	845	11.83	846	11.82
	15	$2LO+LA+TA$	829	12.06	828	12.07
	16	$3LO-LA$	816	12.25	816	12.26
	17	$LO+TO+LA+TA$	810	12.34	809	12.36
	18	$2LO+TO-LA$	797	12.55	795	12.57
	19	$2TO+LA+TA$	791	12.64	792	12.63
	20	$LO+2TO-LA$	778	12.85	778	12.85
E		$2LO+LA$	764	13.09	765	13.07
	21	$3TO-LA$	759	13.17	760	13.15
F		$LO+TO+LA$	745	13.42	745	13.42
	22	$LO+TO+2TA$	743	13.46	741	13.50
G		$2TO+LA$	726	13.77	728	13.73
	23	$2TO+2TA$	724	13.81	725	13.80
	24	$LO+3LA$	712	14.04	712	14.05
	25	$2LO+LA-TA$	699	14.31	700	14.29
H		$2LO+TA$	697	14.35	696	14.36
	26	$TO+3LA$	693	14.43	689	14.52
	27	$LO+TO+LA-TA$	680	14.70	683	14.63
I		$LO+TO+TA$	678	14.75	675	14.83
	28	$2TO+LA-TA$	661	15.13	661	15.12
J		$2TO+TA$	659	15.17	660	15.16

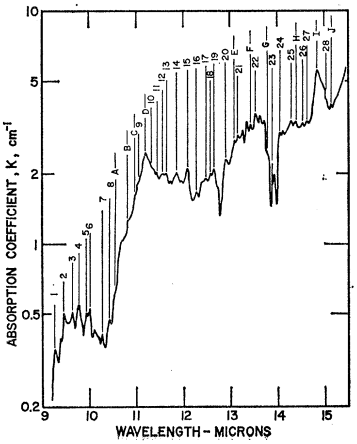

FIG. 3. Absorption coefficient of AlSb vs wavelength at 300°K in the region of three- and four-phonon combination bands. The letters indicate three-phonon bands while the numbers indicate four-phonon bands.

[11] W. G. Spitzer, D. Kleinman, and D. Walsh, Phys. Rev. **113**, 127 (1959).

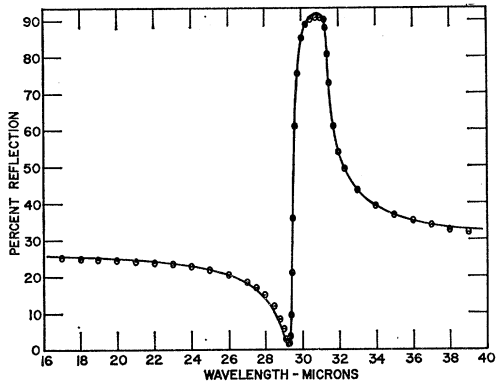

FIG. 4. Reflectivity of AlSb vs wavelength in the Reststrahlen region. The solid curve is the calculated reflectivity, while the points are the experimental data.

where ν_0 is the resonance frequency, $\lambda_0=c/\nu_0$ or resonance wavelength in free space, ρ is a measure of the strength of the resonance, γ governs the width of the resonance, and ϵ_0 is the high-frequency dielectric constant. The definition of γ and ρ are given in reference 10. The errors in ν_0, λ_0, and ϵ_0 were determined from consideration of experimental accuracy in λ and R. The errors in ρ and γ were found by varying these parameters and observing the effect on the fit of reflection data.

Figure 5 shows the index of refraction n, and the extinction coefficient k plotted vs wavelength in microns. These data were obtained from the reflectivity calculation. Figure 6 is a plot of the absorption coefficient K in cm^{-1} vs wavelength in microns for the fundamental Reststrahlen vibration, i.e., the transverse-optical zero wave-vector phonon. The absorption coefficient was calculated from

$$K=4\pi k/\lambda, \tag{10}$$

where k=extinction coefficient from reflectivity calculation and λ=wavelength of light in vacuum.

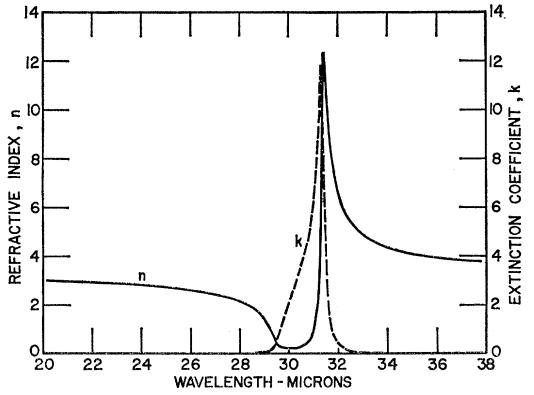

FIG. 5. Index of refraction n and extinction coefficient k of AlSb as functions of wavelength as calculated from the fit of the reflectivity data to simple dispersion theory.

As previously mentioned, the fundamental phonon interaction is by far the strongest lattice band. The value of fundamental phonon TO_c is 319 cm^{-1}. The value of the longitudinal optical frequency at the center of the zone, according to the Lyddane-Sachs-Teller[10] relation is $\nu_1=(\epsilon_\infty/\epsilon_0)^{\frac{1}{2}}\nu_0$, where ϵ_∞ is the low-frequency dielectric constant equal to $\epsilon_0+4\pi\rho$, and ϵ_0 is the high-frequency dielectric constant. With the use of the values given in (9), $\nu_1=10.19\times10^{12}$ sec^{-1} corresponding $LO_c=339.6$ cm^{-1}.

Based on Coulomb attractive forces and nearest-neighbor repulsive forces, Brout[12] has given the sum rule

$$\sum_{i=1}^{6}\omega_i(\mathbf{q})^2=18r_0/\beta m,$$

where β is the compressibility, m the reduced mass, r_0 the interionic distance, and $\omega=2\pi\nu$. Thus the sum of the squares of the lattice frequencies should be a constant for each wave vector $\mathbf{q}$. At the center of the zone

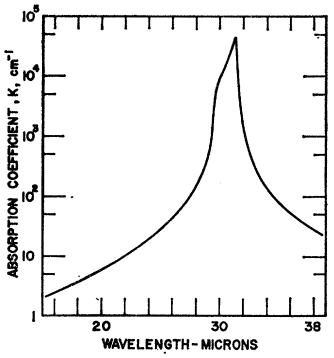

FIG. 6. Absorption of the fundamental lattice vibration in AlSb derived from the extinction coefficient data of Fig. 5.

or $\mathbf{q}=0$,

$$\omega_1^2+2\omega_0^2=1.13\times10^{28}\ sec^{-2}. \tag{12}$$

From the frequencies LO, TO, LA, and TA of Table I, the value of this sum for some $\mathbf{q}$ at or near the zone boundary is

$$\omega_{LO}^2+2\omega_{TO}^2+\omega_{LA}^2+2\omega_{TA}^2=1.08\times10^{28}\ sec^{-2}. \tag{13}$$

In Eqs. (12) and (13) the factors of 2 arise from the assumed degeneracy of the transverse modes. Assuming that (11) holds at the zone boundary, the compressibility is found to be

$$\beta=1.21\times10^{-12}\ cm^2/dyn.$$

The experimental value of β is 1.69×10^{-12} cm^2/dyn.[13] Although the calculated value of β is low and (12) does not equal (13), the values are quite reasonable considering that AlSb is not primarily an ionic crystal and does not therefore fit the assumptions of Brout's rule.

A value of the effective charge $S=0.48$ was calculated

[12] R. Brout, Phys. Rev. **113**, 43 (1959).
[13] D. I. Bolef and M. Menes, J. Appl. Phys. **31**, 1426 (1960).

from the expression given by Born and Huang[14] in terms of the dielectric constants and the fundamental crystal frequency. This value is in agreement with the one reported earlier by Picus *et al.*,[15] although the input data which they used for their calculation were significantly different than the ones reported in this paper.

[14] M. Born and K. Huang, *Dynamical Theory of Crystal Lattices* (Oxford University Press, New York, 1954).
[15] G. Picus, E. Burstein, B. W. Henvis, and M. Hass, J. Phys. Chem. Solids **8**, 282 (1959).

ACKNOWLEDGMENTS

The authors wish to acknowledge the Compound Semiconductor Research Group of Battelle Memorial Institute for the samples of AlSb. We thank R. W. Keyes for his interest and stimulating discussions during the course of the work; W. J. Doherty and R. P. Kelisky who wrote the 7090 program for the reflectivity calculation; and S. P. Keller for his helpful comments on the manuscript.

PHYSICAL REVIEW VOLUME 127, NUMBER 1 JULY 1, 1962

Theory of Photoelectric Emission from Semiconductors

EVAN O. KANE
Bell Telephone Laboratories, Murray Hill, New Jersey
(Received February 23, 1962)

The yield vs energy relation is determined for a number of possible photoelectric production and escape mechanisms involving volume and surface states in semiconductors. Calculations are based on density-of-states considerations and involve energy-band expansions to lowest nonvanishing order about the threshold point. The "direct" and "indirect" processes involving volume states have yields proportional to $E-E_T$ and $(E-E_T)^{\frac{5}{2}}$, respectively. Both processes appear to have been identified experimentally by Gobeli and Allen. The linear yield also requires, in addition to production by "direct" optical excitation, that the observed photoelectrons escape without scattering in the volume or at the surface. Energy and angle distribution functions of the emitted carriers are also determined.

I. INTRODUCTION AND CONCLUSIONS

THE early theoretical work on the photoelectric effect generally made the free-electron approximation for the energy band structure. Fan[1] has given a general quantum mechanical treatment of the volume production of photoelectrons. In his more detailed work he also made the free-electron approximation.

Huntington and Apker[2] have generalized Makinson's[3] work on the surface production of photoelectrons by taking the band structure into account where Makinson assumed "free" electrons with a surface barrier.

The present paper deals primarily with the form of the yield vs energy curve near threshold for a general band structure and for a variety of photoelectron production and scattering mechanisms. These results should be useful in inferring the production mechanism from the yield curve. The principal results are summarized in Table I. The discussion follows the ordering in the table.

In Sec. II the volume production of photoelectrons by "direct" optical transitions is studied. In the absence of volume or surface scattering the yield should be linear with energy, $E-E_d$, above threshold E_d. There is good evidence that this mechanism has been observed by Gobeli and Allen[4] in silicon and by Scheer[5] in CdTe and CdS. This mechanism should produce the highest quantum yields near threshold but it also has the highest threshold energy. The threshold energy will consist of the energy to free the electron, the energy of the hole

TABLE I. Dependence of photoelectric yield, Y, on photon energy, E, near threshold, E_T, for a variety of production and scattering mechanisms. $\mathcal{E}_F$ is the Fermi level measured from the vacuum.

VOLUME PROCESSES	DIRECT OPTICAL EXCITATION	UNSCATTERED		$Y\sim(E-E_T)$
		ELASTICALLY SCATTERED		$Y\sim(E-E_T)^2$
	INDIRECT OPTICAL EXCITATION	UNSCATTERED; ELASTICALLY SCATTERED		$Y\sim(E-E_T)^{5/2}$
SURFACE PROCESSES	VOLUME STATES; SURFACE AS MOMENTUM ABSORBER	"ROUGH" SURFACE		$Y\sim(E-E_T)^{5/2}$
		PERFECT SURFACE		$Y\sim(E-E_T)^{3/2}$
	SURFACE BAND STATES	DIRECT OPTICAL EXCITATION	THRESHOLD $E_T>\lvert\mathcal{E}_F\rvert$	$Y\sim(E-E_T)$
			THRESHOLD $E_T=\lvert\mathcal{E}_F\rvert$	$Y\sim(E-E_T)^{3/2}$
		INDIRECT OPTICAL EXCITATION	$E_T>\lvert\mathcal{E}_F\rvert$	$Y\sim(E-E_T)^2$
			$E_T=\lvert\mathcal{E}_F\rvert$	$Y\sim(E-E_T)^{5/2}$
	SURFACE IMPERFECTION STATES	DISTRIBUTED IN ENERGY; $E_T=\lvert\mathcal{E}_F\rvert$		$Y\sim(E-E_T)^2$
		LOCALIZED IN ENERGY BELOW $\mathcal{E}_F$		$Y\sim(E-E_T)$

[1] H. Y. Fan, Phys. Rev. **68**, 43 (1945).
[2] H. B. Huntington and L. Apker, Phys. Rev. **89**, 352 (1953); H. B. Huntington, *ibid.* **89**, 357 (1953).
[3] R. E. B. Makinson, Phys. Rev. **75**, 1908 (1949).
[4] G. W. Gobeli and F. G. Allen, following paper [Phys. Rev. **127**, 141 (1962)].
[5] J. J. Scheer and J. van Laar, Philips Research Repts. **16**, 323 (1961).